Article

Not peer-reviewed version

Recombinant Production and Functional Characterization of Andes Virus Gn and Gc in Pichia pastoris: A Path Towards Subunit Vaccine Development

Maria Francisca Starck , Claudia Paola Campillay , Belen B.A. Jerez Monsalves , Fátima Reyes , Frank Camacho-Casanova , Jannel Acosta Alba , Raquel Montesino Seguí , Rafael Maura , Fernando J. Ramos-Martínez , Jorge R. Toledo , Oliberto Sánchez Ramos *

Posted Date: 11 October 2024

doi: 10.20944/preprints202410.0828.v1

Keywords: Andes Virus; Pichia Pastoris; recombinant vaccine

 doi:10.20944/preprints202410.0828.v1

Article

Recombinant Production and Functional Characterization of Andes Virus Gn and Gc in *Pichia pastoris*: A Path Towards Subunit Vaccine Development

Francisca Starck [1], Claudia P. Campillay-Véliz [1], Belén Jerez [1], Fátima Reyes [1], Frank Camacho-Casanova [1], Jannel Acosta [2], Raquel Montesino Seguí [2], Rafael Maura [2], Fernando J. Ramos-Martínez [3], Jorge R. Toledo [2,4] and Oliberto Sánchez [1,4,*]

[1] Department of Pharmacology, School of Biological Sciences, University of Concepción, P.O. Box 160C, Concepcion, Chile
[2] Department of Pathophysiology, School of Biological Sciences, University of Concepción
[3] Faculty of Biology, University of Habana, Cuba
[4] Centro de Biotecnología y Biomedicina Spa., Concepción, Chile
* Correspondence: osanchez@udec.cl; Tel.: +56-41-2661191; Fax: +56-41-2203831

Abstract: Hantavirus Pulmonary Syndrome (HPS), caused by the Andes virus (ANDV), is a significant public health concern in South America, with no available vaccines or specific treatments. Neutralizing antibodies targeting ANDV glycoproteins Gn and Gc have shown protective effects in animal models, making them promising vaccine candidates. This study reports the recombinant expression, purification, and immunogenicity evaluation of sGn and sGc glycoproteins produced in the methylotrophic yeast *Pichia pastoris*. Initially, sGn was expressed as a secretable protein, but it formed aggregates once accumulated in the culture medium. To address this, the same strain was transformed with a vector expressing Gc, based on the hypothesis that Gn folding depends on Gc presence. However, co-expression of Gn and Gc in *Pichia* resulted in both proteins becoming trapped as insoluble aggregates inside the yeast, resembling inclusion bodies seen in *E. coli*. The recombinant proteins were solubilized and purified using metal ion affinity chromatography, followed by a refolding step before being used for immunization. The purified sGn and sGc antigens, formulated with aluminum hydroxide (AlOH), were tested in Syrian hamsters. The immunization results showed that the sGn-sGc formulation induced a strong Th1-biased immune response, characterized by high levels of IFN-γ, IL-12, and IL-6 cytokines, along with a specific antibody response against both Gn and Gc, with titers exceeding 1:10,000. These findings suggest the potential of these antigens as promising candidates for a subunit vaccine against HPS.

Keywords: Andes Virus; *Pichia Pastoris*; recombinant vaccine

1. Introduction

The Andes virus (ANDV) is a member of the *Orthohantaviruses* genus (commonly referred to as Hantaviruses) within the *Bunyaviridae* family, is the etiologic agent of Hantavirus Pulmonary Syndrome (HPS) specific to the New World [1]. It primarily affects regions from central to southern Chile, Argentina and southern Uruguay [2–9]. Unlike other pathogenic Hantaviruses, person-to-person transmission has only been documented with ANDV, which has a noteworthy 40% mortality rate [2]. HPS caused by ANDV is characterized by respiratory and hemodynamic failure, typically managed through supportive care provided by healthcare workers [10]. Currently, there is no specific treatment or vaccine approved against ANDV.

ANDV has a tripartite, single-stranded RNA genome with negative polarity (ssRNA (-)) [11]. This genome encodes five major proteins: RNA-dependent RNA polymerase (RdRp), the surface glycoproteins Gn and Gc, the nucleocapsid (N) protein, and a non-structural protein (NSs) [4,7,8,11–

 doi:10.20944/preprints202410.0828.v1

13]. The Gn and Gc glycoprotein complexes play a crucial role in ANDV infection and the development of HPS. These proteins are essential for the hantavirus membrane functions, including the mechanism of viral entry into cells, making them a significant target for therapeutic development [14,15]. Various methodologies have been employed to develop vaccines candidates against HPS. This research has primarily focused on recombinant techniques to develop candidates against the Sin Nombre and Andes viruses. Most of these works has aimed to identify the potential of the surface-exposed glycoproteins Gn and Gc to generate neutralizing antibodies [16–23]. Moreover, research into nucleoprotein-based approaches is also being explored [24–26].

The development of recombinant DNA technology has revolutionized the production of biopharmaceutical proteins, enabling cost-effective manufacturing using various systems. Selecting the optimal expression system requires careful consideration of several factors, including protein productivity, bioactivity, and the physicochemical characteristics of the protein of interest [27]. Additionally, cost, convenience, and safety of the system are crucial factors [27]. Commonly used expression systems included prokaryotic, yeast, insect, and mammalian cells.

Yeasts, like bacteria, offer rapid and inexpensive growth, achieving high cell density in fermenters. Furthermore, they possess more complex post-translational modification pathways, providing advantages such as being non-pyrogenic (fever-free inducing), non-pathogenic (not disease-causing), and capable of efficient protein secretion [28]. The two main yeast systems employed are *Saccharomyces cerevisiae* and the methylotrophic yeast *Pichia pastoris* [29,30]. Methylotrophic yeasts have emerged as particularly attractive alternatives for industrial recombinant protein production due to their promoters controlling gene expression being among the strongest and most tightly regulated in yeast. Furthermore, *P. pastoris* often demonstrates superior performance compared to insect cells or mammalian cells [29].

This study aimed to express, purify, and characterize a recombinant subunit vaccine candidate based on the surface glycoproteins of the Andes virus using the methylotrophic yeast *P. pastoris* as the chosen expression system.

2. Materials and Methods

2.1. Obtaining Recombinant sGn and sGc Antigens Expressed in Pichia Pastoris

2.1.1. Design of antigens based on the exposed regions of the Gn and Gc glycoproteins of ANDV

The design of antigens based on the exposed regions of the Gn and Gc, designated sGn and sGc, utilized the amino acid sequence of the ANDV GPC glycoprotein precursor (NCBI accession number: NP_604472.1). Bioinformatics tools from DTU Bioinformatics (Department of Bio and Health Informatics, Technical University of Denmark) were employed to analyze the precursor sequence. ProP 1.0 predicted the proteolytic site, while TMHMM 2.0 identified transmembrane regions [31,32]. Additionally, SignalP 4.0 and NetNGlyc 1.0 were used to predict signal peptide and potential N-glycosylation sites, respectively [33,34]. Following this analysis, only the exposed regions of both Gn and Gc were retained in their original sequences for antigen design. To enhance protein secretion in the chosen expression system, the *S. cerevisiae* alpha factor secretion signal was added to the N-terminus of each antigen. Additionally, a 7-residue histidine tag was incorporated at the C-terminus to facilitate purification and identification. The nucleotide sequences encoding the final sGn and sGc antigens were then designed based on the optimized amino acid sequences. Codon optimization was performed for efficient expression in the methylotrophic yeast *P. pastoris*. The genes were synthesized by GenScript (People's Republic of China) and cloned into expression vectors: pCBBhis3 for sGn and pCBBz for sGc. The resulting plasmids were named pCBB-sGn and pCBBz-sGc, respectively.

2.1.2. Expression and Purification of sGn Antigen in Pichia Pastoris Using Methanol Induction and Trichloroacetic Acid (TCA) Precipitation

Pichia pastoris strain MP36 served as the host cell for recombinant sGn antigen expression. The vector for transformation was the GenScript-synthesized plasmid pCBB-his3. This plasmid contained

 doi:10.20944/preprints202410.0828.v1

the sGn sequence under the control of the methanol-inducible promoter AOX1. Additionally, it includes the His3 gene expression cassette, which carries the his- mutation specific to strain MP36, enabling selection via auxotrophy. The electrocompetent cells [35] were mixed with pCBB-His3 DNA and subjected to electroporation in a pre-cooled 0.2 cm cuvette using a Micropulser set for the yeast option (BioRad). After pulsing, the cells were recovered with chilled 1M sorbitol for auxotrophic selection. Subsequently, they were transferred to minimal medium (YNB agar) plates for further auxotrophy selection and incubated 3 to 5 days at 30°C. Confirmed transformants were identified using DNA dot blot analysis with a probe specific to the sGn antigen.

Small-scale inductions were performed to assess sGn production by the transformants. A colony was selected from the plates, inoculated into liquid YPG medium and incubated for 2-3 days at 30°C with shaking. This culture was then transferred to a 250 mL flask containing fresh medium and incubated for 24 h at 30°C. The culture was centrifuged at 6000 rpm for 10 minutes (Sorvall, ThermoFisher). The cell pellet was resuspended in 250 mL of YP medium supplemented with 0.5% (v/v) methanol to induce sGn expression. After 12 h, the methanol concentration was increased to 0.75% (v/v), followed by daily additions of 1% (v/v) methanol for to 2 days. The culture was then centrifuged at 8000 rpm for 5 minutes, and both the supernatant (contained the secreted sGn antigen) and yeast pellet were collected. Fractions of interest were stored at -20°C for further analysis. Trichloroacetic acid (TCA) precipitation was used to purify sGn from the supernatant. To the protein sample, 0,1 volume of 0,15% w/v sodium deoxycholate was added. The sample was vortexed, incubated at room temperature for 10 min, and then centrifugated at 8000 g for 20 minutes. The supernatant was discarded, and the sGn-containing pellet was washed with one volume of cold acetone. Following another centrifugation at 8000 g for 5 min, the supernatant was discarded again discarded. The pellet was allowed to air dry at room temperature until the acetone completely evaporated. Finally, the sGn antigen was resuspended in an appropriate volume of sterile distilled water and analyzed using sodium dodecyl sulfate-polyacrylamide gel electrophoresis (SDS-PAGE) on a polyacrylamide gel.

2.1.3. Co-Expression of sGn and sGc Antigens in Pichia Pastoris

The *Pichia pastoris* clone C4-G1, known to express the sGn antigen in the culture medium, was further engineered for co-expression of the sGc antigen. This was achieved through transformation with plasmid pCBBz. This plasmid is a derivative of pCBB-his3, previously used to generate pCBB-sGn for sGn expression. The key difference between the plasmids lies in the selection marker: pCBBz harbors the Sh ble gene, conferring resistance to the antibiotic bleomycin, while pCBB-his3 utilizes the His3 gene. This allows selection of transformants using bleomycin. The transformation methodology employed was identical to that described previously. Following transformation, the capacity of the resulting clones to produce both sGn and sGc antigens was assessed using small-scale inductions. This evaluation followed the same protocol as previously described.

2.1.4. Cell Disruption and Fractionation of Induced Yeast Clones to Measure the Expression of sGn and sGc

Cell disruption and fractionation were performed on the pellets of the induced yeast clones C4-G1, C11-G1+G2, C13-G1+G2 and C41-G1+G2. Briefly, 25 µL aliquots of each pellet were resuspended in 500 µL of yeast genomic DNA purification solution I by vortexing in clean microtubes. Zymolase (2.5 mg/mL) was then added to the mixture and incubated for 1 hour at 37°C. Following centrifugation at 5,000 rpm for 5 min, the supernatant (periplasmic fraction) was transferred to new microtubes. The remaining pellet was resuspended in 100 µL of PBS-Tween 20 (2%) and centrifuged at 10,000 rpm for 5 min. The supernatant (soluble intracellular fraction) was collected in fresh microtubes. Finally, the cell pellet was resuspended in 100 µL of PBS, representing the insoluble intracellular fraction. All three fractions (periplasmic, soluble intracellular, and insoluble intracellular) were subsequently analyzed by SDS-PAGE and western blot.

 doi:10.20944/preprints202410.0828.v1

2.2. Pilot-scale expression, purification and characterization of sGn and sGc antigens in Pichia pastoris

2.2.1. Expression and Rupture of Recombinant sGn and sGc Antigens by Fermentation of Doubly Transformed Pichia Pastoris

The C11-G1+G2 clone was employed to scale up the production of recombinant sGn and sGc antigens. Fermentation was conducted in a 10-liter fermenter equipped with controlled temperature, agitation, aeration, and pH. A two-stage process was employed. Initially, the yeast utilized glycerol as the primary carbon source. Once depleted (approximately 20 hours post-inoculation), methanol was continuously supplied as the carbon source for the remaining fermentation period. The addition of methanol induced the AOX1 gene promoters, thereby driving the expression of sGn and sGc proteins. During the subsequent 96-hour induction phase, a significant increase in biomass (wet weight) was observed, from approximately 45 g/L to 300 g/L. The biomass was then harvested by centrifugation at 8,000 rpm for 10 minutes, separating it from the culture supernatant. The presence of the target antigens within the yeast sample was verified through enzymatic cleavage followed by SDS-PAGE and Western blot analysis. Finally, the harvested biomass was stored at -80°C for further analysis.

The biomass obtained from the previous fermentation of C11-G1+G2 was utilized for cell disruption. Two methods were evaluated for cell disruption efficiency: pressure homogenizer and bead mill. For cell disruption with the pressure homogenizer, the cell pellet was resuspended in sGn-sGc Rupture Buffer at a concentration of 2.5 g/100 mL. The sample was then subjected to 10 homogenization cycles while maintained on ice. Following homogenization, the sample was centrifuged at 5,000 rpm for 30 min at 4°C. The resulting supernatant (soluble fraction) and pellet (insoluble fraction) were collected and analyzed by SDS-PAGE and Western blot. The insoluble fraction, potentially containing the sGn and sGc antigens, was stored at -20°C for further use. For cell disruption with bead mill, the cell pellet was resuspended in sGn-sGc Rupture Buffer at a concentration of 10 g/100 mL. Ten rupture cycles were conducted. The ruptured biomass was collected and centrifuged at 10,000 rpm for 15 min at 4°C. The soluble and insoluble fractions were collected and analyzed by SDS-PAGE and Western blot. The insoluble fraction was stored at a temperature of -20°C until required for use.

2.2.2. Solubilization of Recombinant sGn and sGc Antigens

To solubilize the recombinant sGn and sGc antigens from the insoluble cleavage fraction obtained after cell disruption, various conditions were explored. These conditions included different concentrations of the chaotropic agent urea (0 to 8 M), the reducing agent β-mercaptoethanol (presence or absence of 10 mM), and buffers with a range of pH values (4 to 12). Optimal solubilization was achieved using sGn-sGc Solubilization Buffer, containing 8M Urea, 10 mM β-Mercaptoethanol, and 20 mM NaOH (pH 12). The insoluble cleavage fraction was resuspended in sGn-sGc Solubilization Buffer at a concentration of 2.5 g/100 mL. The suspension was incubated at 45°C for 1 h with vigorous vortexing for 1 min every 15 min. Subsequently, the suspension was centrifuged at 10,000 rpm for 15 min at 4°C. The resulting supernatant (soluble solubilization fraction) and pellet (insoluble solubilization fractions) were collected and analyzed by SDS-PAGE and Western blot. The soluble solubilization fraction was then adjusted to a pH of 8.0 for further use. This adjustment was achieved using 1 M NaH_2PO_4 and HCl, resulting in a final phosphate concentration of 50 mM. The solubilized fraction was finally stored at -20°C until further use.

2.2.3. Purification of sGn and sGc by Metal Ion Affinity Chromatography (IMAC)

Recombinant sGn and sGc antigens were purified using a chromatography column containing 10 mL of Chelating Sepharose Fast Flow® matrix on an ÄKTAstart system. The column was first charged with nickel ions by passing two volumes (10 mL) of 200 mM $NiSO_4$ at a flow rate of 1 mL/min. Subsequently, the column was washed with 100 mL of Milli-Q water to remove unbound nickel ions and then equilibrated with eight volumes (80 mL) of sGn-sGc Equilibration Buffer to

 doi:10.20944/preprints202410.0828.v1

establish a consistent starting condition. The solubilized fraction containing both antigens was loaded onto the equilibrated matrix at a flow rate of 0.5 mL/minute, allowing for specific binding of His-tagged antigens to the nickel ions. Non-adherent proteins were collected in the flow-through fraction. The column was then washed with sGn-sGc Equilibration Buffer until the absorbance at the monitored wavelength returned to baseline, removing nonspecifically bound material. To determine optimal elution conditions, a stepwise imidazole gradient (0 to 500 mM, increasing by 50 mM increments) was applied. Based on the gradient results, the matrix was washed with an optimized sGn-sGc Wash Buffer at a flow rate of 1 mL/min to remove any remaining weakly bound components. Finally, the purified sGn and sGc antigens were eluted using sGn-sGc Elution Buffer at a flow rate of 0.5 mL/min. All collected fractions (flow-through, washes, and eluates) were analyzed by SDS-PAGE with Coomassie blue staining to visualize protein content and identify fractions containing the purified antigens. Western blotting was performed to confirm the presence and purity of the sGn and sGc antigens. Following confirmation of purity, the recombinant antigen(s) were quantified using appropriate methods.

2.2.4. Refolding of sGn and sGc by Ultrafiltration

The elution fraction obtained from IMAC purification was used for the refolding and analysis of sGn and sGc antigens. The refolding process was carried out in parallel with ultrafiltration using a 20-mL Amicon Bioseparations Stirred Cells ultrafiltration system (Merck, Germany) equipped with a 5-kDa Ultracell ultrafiltration disk (Merck, Germany). The system was connected to a P1 pump, and the refolding buffer (sGn-sGc Replenishment Buffer) was introduced at a flow rate of 50 µL/min at 16°C. Four to five volumes of refolding buffer were exchanged with the eluted fraction, followed by a buffer change to sGn-sGc immunization buffer (four to five volumes) without disconnecting the system. The final refolded sample was extracted, supplemented with 0.02% (v/v) Tween 20 was, and analyzed by SDS-PAGE with Coomassie Blue staining and Western Blotting. Following analysis, the recombinant antigen(s) were quantified and stored in 1 mL aliquots at - 80ºC until further use.

2.3. Immunological Validation of Recombinant Antigens

2.3.1. Vaccinal Formulations

Four vaccine formulations were prepared for immunization assays, incorporated either Freund's incomplete adjuvant (FIA) or aluminum hydroxide (AlOH) as adjuvants. The formulations were as follows:

- Formulation 1: FIA + PBS (1:1)
- Formulation 2: AlOH + PBS (1:1)
- Formulation 3: sGn/sGc-FIA (20 µg) (1:1)
- Formulation 4: sGn/sGc-AlOH (20 µg) (1:1)

2.3.2. Animals and Experimental Design

Twenty female Syrian hamsters (8-10 weeks old) were used in this study. Animals were randomly assigned to four experimental groups (five hamsters per group) and housed individually in cages under identical conditions with *ad libitum* access to water and food. The animal room was maintained at 25°C in rooms with filtered air and 12-hour light/dark cycle. All procedures adhered to the ethical standards approved by Bioethics Committee of the Faculty of Biological Sciences of the Universidad de Concepción.

Each group received one of the four vaccines formulations described above. Immunizations were administered subcutaneously in the dorsal region with 100 µL volume on days 1, 21, and 42. Blood samples were collected weekly until day 63 (week 9). On day 63, the animals were euthanized, and their splenocytes were collected for the evaluation of the cellular immune response.

 doi:10.20944/preprints202410.0828.v1

2.3.3. Blood Collection

Blood samples were collected weekly from each hamster throughout the study period. Prior to collection, animals were anesthetized with isoflurane for minimal stress. Approximately 300-500 µL of blood was collected from the retro-orbital vein using heparinized capillary tubes. Following collection, blood samples were transferred to microtubes and centrifuged at 8,000 x g for 15 minutes. The resulting plasma was aspirated, aliquoted into clean microtubes, and stored at -20°C until further analysis.

2.3.4. Quantification of Total IgG Antibodies by Enzyme-Linked Immunosorbent Assay (ELISA)

The levels of total IgG antibodies specific for sGn/sGc antigens were determined by ELISA as previously described [36]. Briefly, the target antigen was diluted to 10 µg/mL in coating buffer and used to coat high-binding 96-well plates at 1 µg per well. The plates were incubated overnight at 4°C in a humidified chamber. The following day, the coating buffer was discarded, and the plates were washed twice with phosphate-buffered saline containing Tween-20 (PBS-T) to remove unbound antigen. Subsequently, the plates were blocked with 3% bovine serum albumin (BSA) in PBS for 2 hours at 37°C in a humidified chamber. Following three washes with PBS-T, serial dilutions of plasma samples collected from immunized hamsters were added to the wells and incubated for 2 hours at 37°C in a humid chamber. Unbound antibodies were removes by washing the plates. Then, HRP-conjugated anti-hamster secondary antibody was added to each well and incubated for 1 hour at 37°C in a humidified chamber. After another washing step, the plates were incubated with a substrate solution containing o-phenylenediamine and hydrogen peroxide for 20 minutes at room temperature in the dark. The enzymatic reaction was stopped by adding sulfuric acid 2,5 M to each well. The absorbance of the samples was measured at 492 nm using the Spectro Star NANO plate reader (BMG LabTech, Germany). The assay was performed in triplicate for each sample. Wells with an OD value two or more times higher than the corresponding day zero OD for the same dilution within the same experimental group were considered positive for specific antibody response.

2.3.5. Evaluation of the Cytokine Profile of Splenocytes

Splenocytes were isolated from euthanized hamsters and seeded into 24-well plates. Half of the wells for each animal received stimulation with the sGn/sGc antigenic complex at a concentration of 1 µg/mL for 24 hours, while the remaining wells served as unstimulated control. After 24 hours of incubation, splenocytes were processed using the RNeasy Micro Kit (Qiagen, USA) following the manufacturer's instructions. Purified RNA was used to evaluate the relative expression of T helper lymphocyte profile-associated cytokines (IFN-γ, IL-12, IL-4, and IL-6) using the Power SYBR Green Cells-to-CT kit (ThermoFischer Scientific, USA). Specific Oligonucleotides for the target genes (Supplementary Table S1) were employed, with the ribosomal protein L18 as a housekeeping gene for normalization. Quantitative PCR (qPCR) was performed on an AriaMx 96 Real-Time PCR System (Agilent). The relative differences in RNA levels of each cytokine between stimulated and unstimulated splenocytes were determined using the 2-ΔΔCt method [37,38].

3. Results

3.1. Design, Expression and Purification of a Soluble Variant of the ANDV Gn Glycoprotein in Pichia Pastoris

The soluble variant of the ANDV Gn glycoprotein, named sGn, was designed based on the amino acid sequence of GPC (UniProtKB ID: Q9E006) from ANDV strain Chile-971786. Bioinformatics tools predicted the proteolytic site of the precursor, transmembrane regions, signal peptide, and potential N-glycosylation sites [31–34]. Exposed regions of the Gn sequence were retained for sGn design. To facilitate purification and identification, the secretion signal of *S. cerevisiae* alpha factor and a 7-residue histidine tag were added at the N-terminus and C-terminus of sGn, respectively. The theoretical molecular weight and isoelectric point of the designed protein were

 doi:10.20944/preprints202410.0828.v1

predicted to be 44.3 kDa and 6.45, respectively. Codon-optimized for expression in the methylotrophic yeast *P. pastoris*, the sGn gene was constructed and inserted into the pCBB-his3 plasmid for expression under the control of the AOX-1 promoter. The resulting plasmid, pCBB-sGn (Supplementary Figure S1B), was transformed into *Pichia pastoris* strain MP36. Recombinant clones were identified by auxotrophy and confirmed by DNA dot blot using a Gn sequence fragment as a probe (Supplementary Figure S1A). Positive clones, designated C4-G1 and C5-G1 were subjected to small-scale induction.

As anticipated due to the engineered absence of transmembrane regions and the inclusion of a secretion signal, the recombinant sGn antigen was secreted into the culture medium. Following induction, the culture medium was collected, and proteins were precipitated using the TCA method. SDS-PAGE under reducing and non-reducing conditions (Figure 1A), followed by western blotting with an anti-Gn monoclonal antibody, confirmed sGn expression by both clones (Figure 1B). However, these assays also revealed the formation of heterogeneous aggregates with different molecular weights, some larger than 245 kDa.

To address the observed heterogeneity of the sGn antigen in the *P. pastoris* culture medium, a density gradient separation assay was performed using a 10%-80% sucrose gradient (Figure 1C). This aimed to identify the density of different sGn antigen fractions and facilitate purification of a specific fraction. Fractions were collected and analyzed by protein dot blot using an anti-Gn monoclonal antibody. The analysis indicated a homogeneous distribution of the antigen across a density range of 1,15-1,45 kg/m³, confirming the formation of aggregates with varying molecular weights and densities.

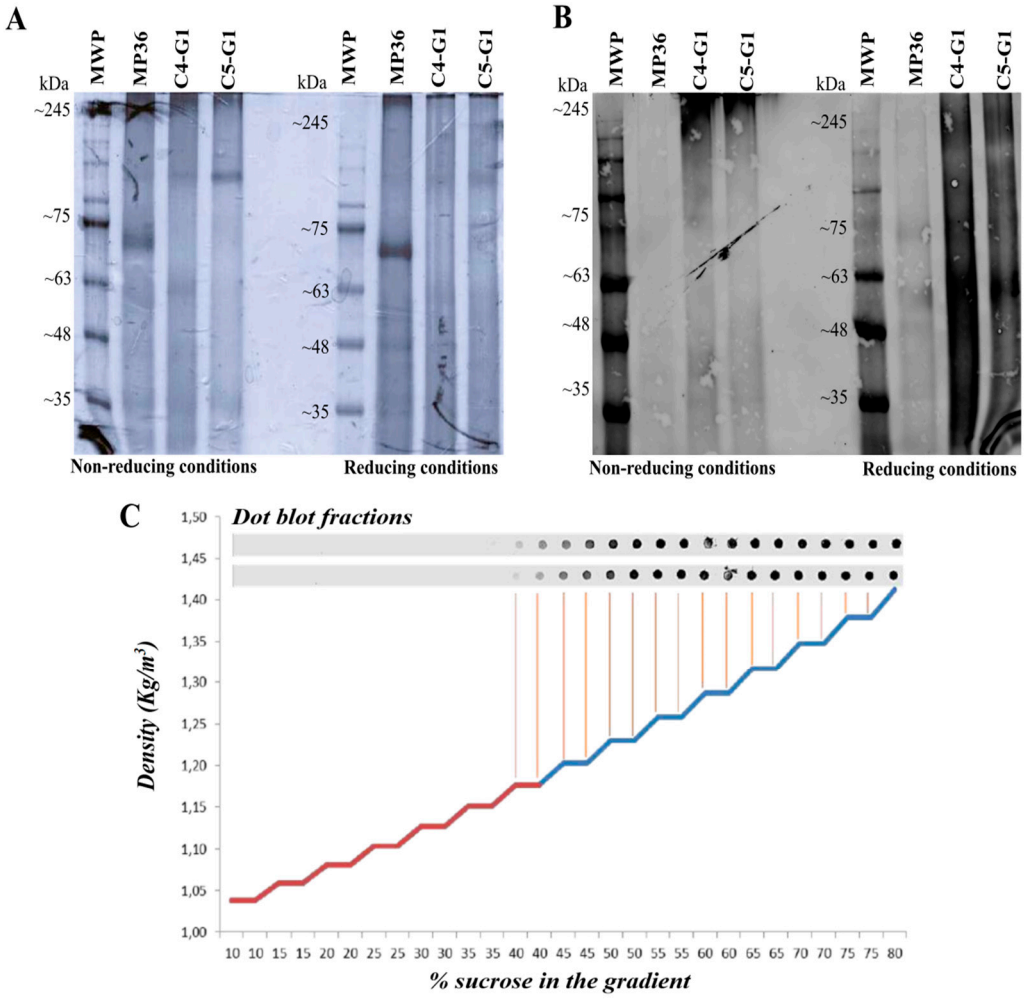

Figure 1. The sGn antigen forms heterogeneous aggregates with different molecular weights and densities: (**A**) SDS-PAGE of the induction supernatant of clones C4-G1 and C5-G1 under non-

 doi:10.20944/preprints202410.0828.v1

reducing and reducing conditions. (**B**) Western blot of the induction supernatant of clones C4-G1 and C5-G1 under non-reducing and reducing conditions. (**C**) Density analysis of the multimers found when expressing sGn. The presence of sGn in the different fractions of a saccharose gradient from 10% to 80% is plotted. ***MWP.*** *Molecular weight pattern.* ***MP36****. Induction supernatant of the native strain MP36.* ***C4-G1****. Induction supernatant of clone C4-G1.* ***C5-G1****. Induction supernatant of clone C5-G1.*

3.2. Design and Co-Expression of the Soluble Variant of the ANDV Gc Glycoprotein in the C4-G1 Pichia Pastoris Clone

The purification challenges posed by heterogeneous conformations of recombinant sGn antigen necessitated a new approach. This decision was based on the established tendency of hantavirus surface glycoproteins form homo- and hetero-oligomers, creating a lattice-like structure on the viral surface. To target both ANDV surface glycoproteins, a vector was designed for expression of the exposed regions of the ANDV Gc glycoprotein, designated sGc. Similar to the sGn construct, the sGc design incorporated the alpha factor secretion signal and a histidine tag for efficient purification and identification. The theoretical molecular weight and isoelectric point of sGc were predicted to be 51,2 kDa and 6,27, respectively. Codon optimization for *P. pastoris* expression was considered during the design of the sGc nucleotide sequence.

The designed sGc gene was cloned into the *P. pastoris* expression vector pCBBz, a derivative of the pCBB-his3 plasmid. Notably, pCBBz replaces the His3 gene with the Sh ble gene, conferring resistance to bleomycin and enabling antibiotic selection of recombinant clones. The resulting plasmid was named pCBBz-sGc (Supplementary Figure S2A).

To achieve co-expression of both sGn and sGc antigens, clone C4-G1 was re-transformed with the pCBBz-sGc plasmid. Recombinant clones were selected based on their ability to growth on zeocin-containing solid medium, followed by growth in liquid medium under selective pressure. Post-induction with methanol, the presence of both antigens in the induction culture medium was assessed. Proteins were precipitated using the TCA method, and SDS-PAGE was performed under reducing conditions followed by Western blot analysis using anti-Gn and anti-Gc monoclonal antibodies (Supplementary Figure S2).

Interestingly, while the C4-G1 clone continued to express sGn (Supplementary Figure S2C), the recombinant clones were unable to secrete sGc into the culture medium (Supplementary Figure S2D). Furthermore, a significant proportion of the doubly recombinant clones (C11, C13, C44, C66, C78, and C86) also failed to secrete recombinant sGn (Supplementary Figure S2C). These observations led us to hypothesize that the absence of both antigens in the medium might be due to sGc expression within the yeast, potentially causing retention of the sGn as well.

To investigate this possibility, the yeasts pellet obtained from the induction of the doubly recombinant clones (C11-G1 + G2, C13-G1 + G2, C41-G1 + G2) and the initial induction of clone C4-G1 were lysed. Periplasmic, intracellular soluble, and intracellular insoluble fractions were analyzed separately for each clone (Supplementary Figure S3). These analyses revealed that the doubly recombinant clones were indeed capable of expressing both antigens. However, both recombinant proteins were retained within the yeast.

Based on these findings, we opted to continue working with the C11-G1+G2 clone due to its apparently higher expression levels of both antigens. This observation is consistent with the stronger band observed in the Coomassie blue-stained polyacrylamide gel (Supplementary Figure S3A, lane 7), which aligns with the signals in the Western blot assays (Supplementary Figure S3B,C, lane 7).

3.3. Production and Characterization of Recombinant sGn and sGc Antigens

The co-expression of sGn and sGc antigens in clone C11-G1+G2 was confirmed following induction in 10 L a pilot-scale fermenter. The fermentation pellet was analyzed using specific monoclonal antibodies against each of the ANDV surface glycoproteins (Figure 2A). This analysis established the need for further processing to solubilize the recombinant antigens. Initial attempts employed a urea gradient for solubilization of the insoluble fraction obtained from the fermentation pellet. The soluble and insoluble fractions after treatment with various urea concentrations were

 doi:10.20944/preprints202410.0828.v1

analyzed by SDS-PAGE and Western blot under reducing conditions (Supplementary Figure S4). To optimize solubilization, a series of additional buffers were evaluated, incorporating varying pH and β-mercaptoethanol as a reducing agent. These conditions were compared by SDS-PAGE and Western Blot under both reducing and non-reducing conditions (Supplementary Figure S5). The results indicated 8 M urea and 10 mM β-mercaptoethanol were most effective for solubilization. Following solubilization, a purification protocol using IMAC was developed. A stepwise imidazole gradient was applied and each collected fractions was subjected to SDS-PAGE and Western blot analysis. Based on these results, optimal conditions for sample loading, washing, and elution of the recombinant antigens were determined to be 5 mM, 50 mM, and 200 mM imidazole, respectively. Urea and β-mercaptoethanol were maintained in all buffers throughout the purification process. The purified fractions were subsequently analyzed by SDS-PAGE and Western blot (Figure 2B,C).

Densitometric analysis of SDS-PAGE gels indicated a purity level of 98% for the recombinant antigens. The yield of the production process was approximately 2 grams of antigen per liter of fermentation broth (2 g/L).

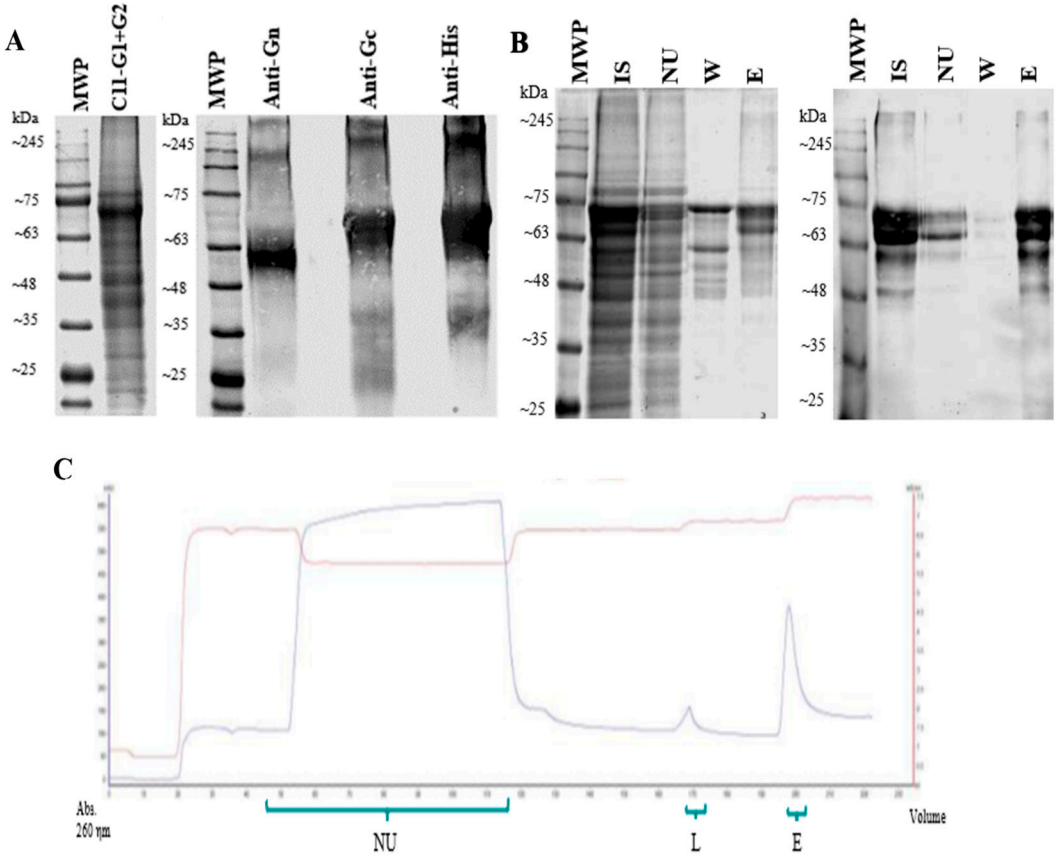

Figure 2. Purification of solubilized recombinant sGn and sGc antigens: (**A**) SDS-PAGE and Western Blot of the soluble fraction of the fermentation pellet of clone C11-G1+G2. (**B**) SDS-PAGE and Western Blot in reducing conditions of the purification process by IMAC. (**C**) Chromatogram of the purification process by IMAC, indicating absorbance at 260 ηm in blue and conductivity in red. ***MWP.*** *Molecular weight pattern.* ***IS.*** *Solubilized fraction containing sGn and sGc antigens (input sample).* ***NU.*** *Non-Unbound fraction.* ***W.*** *Washed fraction.* ***E.*** *Eluted fraction.*

Refolding of the purified proteins was performed using the elution fraction from the IMAC. The refolding procedure involved a drip buffer change and concentration. The protein status before and after refolding was analyzed by SDS-PAGE and Western Blot under both non-reducing and reducing conditions (Supplementary Figure S6A,B). Analysis of the refolded antigens revealed the formation of high molecular weight aggregates exceeding 245 kDa. It is possible that some of these aggregates

 doi:10.20944/preprints202410.0828.v1

are too large the separating gel during electrophoresis, resulting in their retention within the staking gel.

To further characterize the recombinant antigens, post-refolding samples were analyzed by SDS-PAGE and Western Blot using specific antibodies against ANDV Gn and Gc glycoproteins (Supplementary Figure S6C). This analysis confirmed the presence of both antigens after purification and refolding processes.

The occupancy of potential N-glycosylation sites in both antigens (four in the Gn-based antigen and one in the Gc-based antigen) was investigated using a deglycosylation assay. The products were analyzed by SDS-PAGE and Western blot with specific antibodies against ANDV Gn and Gc glycoproteins. The results suggest that the N-glycosylation site in the Gc-based recombinant antigen is occupied, while none of the potential N-glycosylation sites in the Gn-based antigen appear to be glycosylated (Supplementary Figure S7).

3.4. Evaluation of the Immunogenicity of Recombinant sGn-sGc Antigens in Syrian Hamsters

The production of total IgG antibodies against the vaccine antigens were evaluated by ELISA. Hamsters in Group D (Formulation 4: sGn/sGc-AlOH) exhibited the earliest antibody development, starting in the second week post-vaccination (Figure 3D). In contrast, Group C (Formulation 3: sGn/sGc-FIA) showed delayed antibody response, beginning in the fourth week (Figure 3C). Antibody titers generally increased following each immunization on days 21 and 42. On day 63, the Group C achieved average titer of 1/9,200 (13.17 ± 1.27 Log2) while Group D achieved the highest average titer of approximately 1/7,300 (12.84 ± 1.29 Log2) (Figure 3C,D). Given the superior performance of Group D throughout the study, subsequent analyses were focused on this group.

To assess the cellular immune response, splenocytes from immunized hamster from Group D were isolated and stimulated with the Gn and Gc antigenic complex. The relative mRNA levels of IFN-γ, IL-12, IL-4, and IL-6 were evaluated by RT-qPCR. Stimulated splenocytes exhibited significant increases in IFN-γ (Figure 3E), IL-12 (Figure 3F), and IL-6 levels (Figure 3H), indicative of Th1-biased immune response. Notably, IL-4 levels remained unchanged, suggesting a lack of Th2 response (Figure 3G).

 doi:10.20944/preprints202410.0828.v1

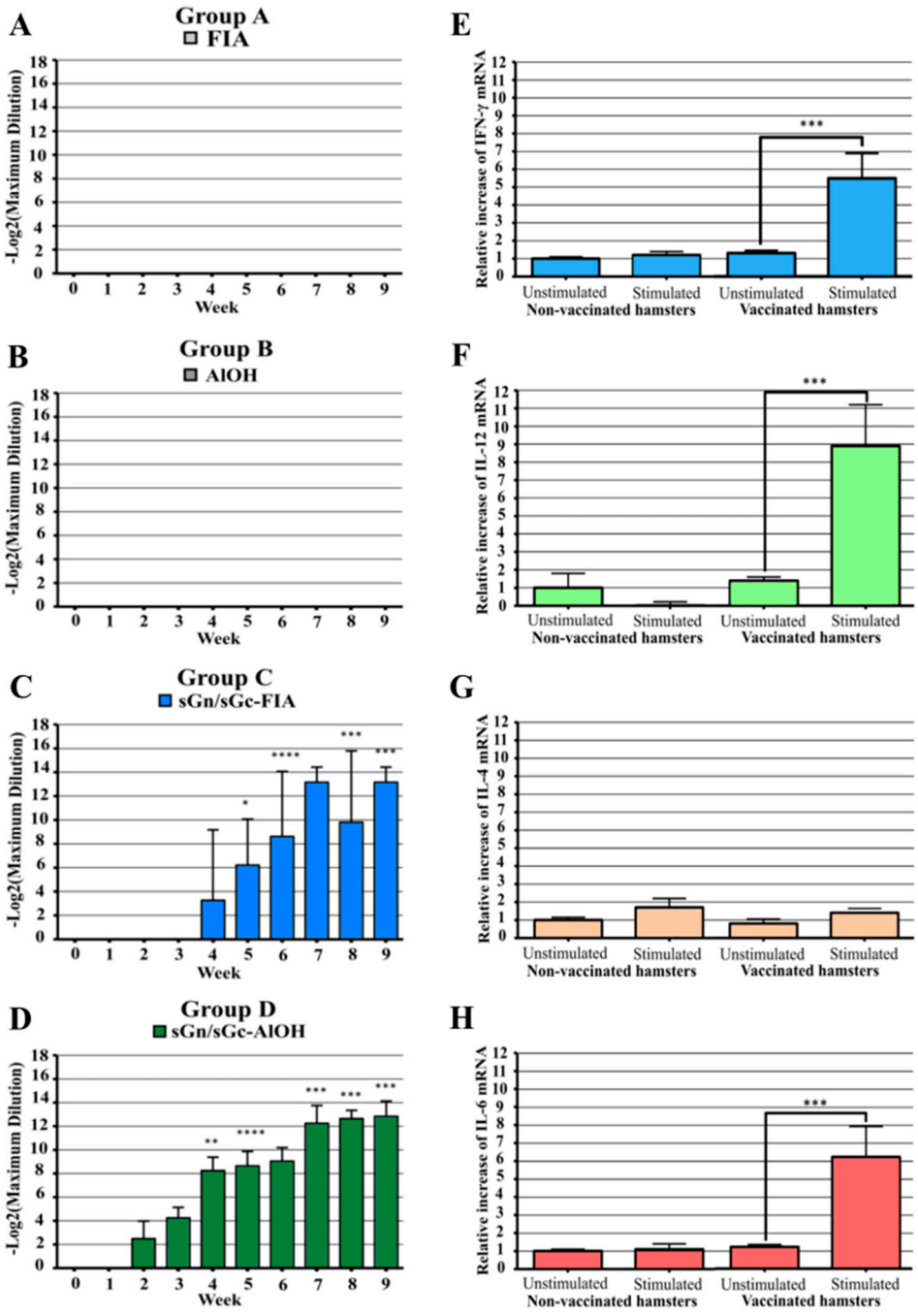

Figure 3. Immunization with AlOH-adjuvanted sGn/sGc antigens induces the production of IgG antibodies and cytokines involved in a Th1-type response profile in Syrian hamsters: (A) Total IgG antibody titers in group A immunized with FIA + PBS (1:1). (B) Total IgG antibody titers in group B immunized with AlOH + PBS (1:1). (C) Total IgG antibody titers in group C immunized with sGn/sGc-FIA (20 μg) (1:1). (D) Total IgG antibody titers in group D immunized with sGn/sGc-AlOH (20 μg) (1:1). (E) Relative levels of interferon gamma RNA in splenocytes of Syrian hamster immunized with the sGn/sGc-AlOH formulation. (F) Relative levels of IL-12 RNA in splenocytes of Syrian hamster immunized with the sGn/sGc-AlOH formulation. (G) Relative levels of IL-4 RNA in splenocytes of Syrian hamster immunized with the sGn/sGc-AlOH formulation. (H) Relative levels of IL-6 RNA in splenocytes of Syrian hamster immunized with the sGn/sGc-AlOH formulation. *In graphs A, B, C and D the values represent mean ± SE. (two-way ANOVA, followed by Dunnet's multiple comparison test; **, p<0.01; ***, p<0.001; ****p<0.0001). In graphs E, F, G and H the values represent the mean ± SE. (Two-way ANOVA, followed by Bonferroni multiple comparison test; ****p<0.0001).*

 doi:10.20944/preprints202410.0828.v1

4. Discussion

This study aimed to develop recombinant antigens based on the Gn and Gc glycoproteins of ANDV for expression in yeast, addressing the challenges associated with low soluble antigen production in mammalian cell systems [39]. Initially, attempts to co-express both antigens in yeast using a single construct were unsuccessful. Consequently, the focus shifted to the generation yeast clones capable of producing individual antigens. Two clones successfully secreted a recombinant antigen based on the exposed regions of the ANDV Gn glycoprotein, designated sGn. However, contrary to expectations, sGn formed aggregates of varying molecular weights (Figure 1), suggesting a requirement for co-expression with Gc for proper folding and higher-order structures formation, consistent with previous findings [40–43]. Furthermore, studies have demonstrated the association between glycoproteins of the same type (Gn-Gn and Gc-Gc interactions) in hantaviruses [44,45]. These aggregation issues hindered purification and subsequent vaccine development efforts.

To address these challenges, the C4-G1 clone (expressing sGn) was re-transformed with a plasmid encoding the sGc antigen. While both antigens were expressed, they were unexpectedly retained within the yeast cell rather than being secreted into the culture medium. This phenomenon was attributed to the formation of high molecular weight aggregates within the yeast, resulting from interactions between sGn and sGc. Analysis of cellular fractions confirmed the intracellular expression of both antigens but their retention within the cell (Supplementary Figures S2 and S3). The observed aggregation is consistent with the known interaction between Gn and Gc glycoproteins in the native virus, forming a specific pattern on the viral surface [41,43,46]. While these findings suggest a potential link between the aggregation of recombinant antigens and their native conformation, further investigations are required to substantiate this hypothesis.

Solubilization of the recombinant sGn and sGc antigens necessitated the use of harsh conditions, including high concentrations of chaotropic agent, reducing agents, alkaline pH, and heat treatment (Supplementary Figures S4 and S5). Despite these measures, a significant portion of the high-molecular-weight aggregates persisted, indicating a robust interaction between the two antigens. Nonetheless, the antigens were successfully purified to a high degree of purity (>95%) with minimal loss during the process (Figure 2). Subsequent refolding of the antigens was crucial for preserving both linear and conformational epitopes, essential for the development of an effective vaccine candidate.

The refolding process was evaluated by comparing the electrophoretic mobility before and after refolding under non-reducing conditions (Supplementary Figure S6). A shift from monomeric bands to high-molecular-weight aggregates was observed, accompanied by solution turbidity. Despite their size, these aggregates remained soluble and filterable through 0,22 μm filters, indicating the absence of virus-like particle (VLP) formation. Previous studies have demonstrated VLP formation upon transfection of mammalian cells with full-length Gn and Gc glycoproteins [47], suggesting that the deleted regions in our design, particularly the transmembrane regions, are crucial for VLP assembly but not for the interaction between both glycoproteins. To elucidate the structural conformation of the refolded sGn and sGc antigens, further analysis is required to determine or estimate their folding patterns. Comparative analysis with existing structural data on hantavirus glycoproteins would provide valuable insights. Moreover, the preservation of epitopes, as previously mapped on the surface of ANDV and other hantaviruses [48,49], should be evaluated to assess the antigenicity of the refolded proteins. These studies are crucial to evaluate the potential of the refolded antigens as vaccine candidates.

To assess the occupancy of potential N-glycosylation sites, the recombinant antigens were subjected to deglycosilation analysis. Results indicated that sGn lacked glycosylation at all predicted sites, while sGc exhibited occupancy of its sole N-glycosylation site (Supplementary Figure S7). Interestingly, two distinct bands were observed for the sGc antigen (Supplementary Figure S7C) suggesting heterogeneity in the presence or absence of the secretion signal rather than glycosylation differences. The molecular weights of both recombinant antigens, as determined by Western blot, align with theoretical predictions. Although some studies have highlighted the importance of glycosylation for proper folding of Gn and Gc glycoproteins [50], other research has demonstrated

 doi:10.20944/preprints202410.0828.v1

the ability of proteins to adopt correct conformations without native glycosylation patterns [51,52]. Given characteristics of our recombinant antigens, including their scalability and production efficiency, we propose that these antigens hold potential as vaccine candidate.

Finally, to assess the immunogenicity of the recombinant sGn-sGc antigens, a vaccination scheme consisting of a primary immunization followed by two booster doses was administered to Syrian hamsters. This immunization protocol was selected based on its efficacy in human vaccine trials utilizing recombinant antigens, including yeast-produced surface proteins [53,54]. Two distinct adjuvants, Freund's incomplete adjuvant (FIA) and aluminum hydroxide (AlOH), were employed to evaluate their impact on antigen immunogenicity. FIA, extensively characterized in experimental and veterinary settings, is known to induce a robust Th1-type immune response [55], a desirable profile for combating intracellular pathogens like ANDV. While not currently approved for human use, other oil-in-water adjuvants such as MF59 could be explored in future studies [56]. AlOH, a widely used aluminum salt-based adjuvant in human vaccines [57,58], typically elicits antibody-mediated immune responses, primarily associated with protection against extracellular pathogens in murine models. However, its efficacy in inducing protective immunity against intracellular pathogens, including demonstrated success in Hepatitis B and Human Papillomavirus vaccines, warranted its inclusion in this study [53,59,60].

The Syrian hamster was selected as the animal model for HPS due to its established susceptibility to ANDV infection. As HPS in exclusively induced by ANDV or non-pathogenic Maporal virus in humans, the hamster model offers a valuable tool for developing treatments and vaccines against this disease [61,62]. Additionally, the Syrian hamster exhibits immune responses to pathogens that closely resemble those observed in humans [63]. However, limitations inherent to animal models must be acknowledged. While the hamster model provides valuable insights, its immune response may not fully recapitulate human immune responses, particularly in terms of antigen processing and presentation. Furthermore, genetic variability among individual hamsters can introduce experimental variability. Therefore, the results obtained in this study should be interpreted within the context of these limitations. As expected, control groups in the total IgG antibody titer evaluation exhibited no significant increase (Figure 3). In contrast, groups immunized with recombinant sGn-sGc antigens displayed higher total IgG titers. Both groups (FIA and AlOH adjuvants) reached comparable peak titers by day 63 (last sample collection): 1/9,200 (13.17 ± 1.27 Log2) and 1/7,300 (12.84 ± 1.29 Log2), respectively. These results suggest potential use of AlOH as a human vaccine adjuvant due to its established safety profile [58]. Consequently, further analysis focused solely on samples from the sGn/sGc-AlOH group. To assess the cellular immune response, the relative mRNA expression levels of IFN-γ, IL-12, IL-4, and IL-6 were evaluated in splenocytes (Figure 3E–H). These cytokines are key indicators of Th1 and Th2 lymphocyte profiles [64–68]. A significant increase in IFN-γ and IL-12 mRNA levels was observed, suggesting a predominantly Th1-type response. While elevated IL-6 levels were also detected, the pleiotropic nature of this cytokine precludes definitive interpretation. Due to the limited scope of this study, focusing on a small panel of cytokines and a single time point post-stimulation, the observed cytokine profile provides preliminary insights rather than a comprehensive characterization of the immune response. Further studies should be including a more extensive cytokines analysis at multiple time points to elucidate the complete immune response dynamics induced by the vaccine candidate. Additionally, assessment of other immune parameters, such as cytotoxic T lymphocytes activation and antibody-dependent cellular cytotoxicity, is warranted for a deeper understanding of the vaccine's efficacy. Additionally, exploring the use of alternative adjuvants, such as those incorporating of immunopotentiators, may enhance vaccine formulation [69,70]. Other critical factors, including the optimal route of administration [71], long-term immune response evaluation, and challenge studies to assess protection against ANDV infection, must be addressed in future studies.

5. Conclusions

This study demonstrated the ability of recombinant antigens derived from the exposed regions of Andes virus Gn and Gc glycoproteins, produced in *Pichia pastoris*, to induce a specific immune

 doi:10.20944/preprints202410.0828.v1

response in Syrian hamsters. The antigens were purified to high purity (approximately 98%) with a yield of 2 grams per liter of fermentation broth. When formulated with aluminum hydroxide, these antigens elicited a robust immune response characterized by elevated total IgG antibody titers (1 in 7,300) and a predominantly Th1-type cytokine profile (increased IFN-γ, IL-12, and IL-6 levels). These findings are particularly noteworthy as Th1 responses are typically associated with intracellular pathogens like viruses.

6. Patents

A patent application (WO/2020/034048) was filed by the Centro de Biotecnología y Biomedicina SPA on August 13, 2019, describing a novel vaccine against hantavirus cardiopulmonary syndrome. This patent, PCT/CL2019/050072, outlines a promising approach for the prevention of this severe disease.

Supplementary Materials: The following supporting information can be downloaded at: https://www.preprints.org/, Figure S1: Dot blot of DNA from yeast clones transformed with plasmid pCBB-sGn; Figure S2: SDS-PAGE and Western Blot of the induction supernatant of clones obtained by re-transformation of C4-G1 with pCBBz-sGc; Figure S3: SDS-PAGE and Western Blot of the intracellular fractions of the clones obtained by re-transformation of C4-G1 with pCBBz-sGc, after induction; Figure S4: Soluble and insoluble fractions after urea solubilization of the insoluble fraction of the fermentation pellet breakdown of clone C11-G1+G2; Figure S5: Soluble and insoluble fractions after solubilization optimization; Figure S6: Characterization of recombinant antigens sGn and sGc under different conditions of purification; Figure S7: Occupancy analysis of potential N-glycosylation sites in the recombinant antigens; Table S1: Primers used for the evaluation of changes in relative cytokine mRNA levels in hamsters by qPCR.

Author Contributions: Conceptualization, O.S., F.S., and J.R.T.; methodology, F.S., F.R., F.C., R.M., J.A., and R.M.; validation, O.S., and J.R.T.; formal analysis, B.J., F.J.R-M. and C.P.C-V.; investigation, O.S., F.S., J.R.T., F.R., F.C., J.A., and R.M.; resources, O.S., and J.R.T.; writing—original draft preparation, C.P.C-V., F.J.R-M. and B.J.; writing—review and editing, O.S.; supervision, O.S., and J.R.T.; project administration, O.S.; funding acquisition, O.S. All authors have read and agreed to the published version of the manuscript.

Funding: This research was funded by the Centro de Biotecnología y Biomedicina Spa. (CBB), Corporación de Fomento a la Producción (CORFO) through co-funding projects 17IDAE-74735, and the National Agency of Research, ANID, Chile through National Doctoral Scholarship No. 21221600.

Institutional Review Board Statement: The study was conducted in accordance with the Declaration of Helsinki and approved by the Ethics Committee) of Facultad de Ciencias Biológicas, Universidad de Concepción (protocol CEBB-047-2018, and date of approval January 16, 2018.).

Data Availability Statement: The authors confirm that the data supporting the findings of this study are available within the article and its supplementary materials.

Acknowledgments: The authors would like to thank Manuel Iturra and Claudio Bastía for their help and support in technical lab work.

Conflicts of Interest: The authors declare no conflicts of interest.

References

1. Maes, P., et al., *Taxonomy of the family Arenaviridae and the order Bunyavirales: update 2018*. 2018, Springer-Verlag Wien. p. 2295-2310.
2. Martinez, V.P., et al., *Person-to-Person Transmission of Andes Virus*. 2005, Centers for Disease Control and Prevention. p. 1848.
3. Avšič-Županc, T., A. Saksida, and M. Korva, *Hantavirus infections*. 2019, Elsevier. p. e6-e16.
4. Bi, Z., P.B.H. Formenty, and C.E. Roth, *Hantavirus Infection: a review and global update*. 2008. p. 003-023.
5. Jonsson, C.B., J. Hooper, and G. Mertz, *Treatment of hantavirus pulmonary syndrome*. 2008, Elsevier. p. 162-169.
6. MacNeil, A., S.T. Nichol, and C.F. Spiropoulou, *Hantavirus pulmonary syndrome*. 2011, Elsevier. p. 138-147.
7. McCaughey, C. and C.A. Hart, *Hantaviruses*. 2000, Lippincott Williams and Wilkins. p. 587-599.
8. Muranyi, W., et al., *Hantavirus infection*. 2005. p. 3669-3679.
9. Vinh, D.C. and J.M. Embil, *Hantavirus pulmonary syndrome: a concise clinical review*. 2009. p. 620-625.

10. Castillo, C., et al., *Hantavirus Pulmonary Syndrome Due to Andes Virus in Temuco, Chile: Clinical Experience With 16 Adults*. 2001, Elsevier. p. 548-554.
11. Plyusnin, A., O. Vapalahti, and A. Vaheri, *Hantaviruses: Genome structure, expression and evolution*. 1996, Microbiology Society. p. 2677-2687.
12. Hepojoki, J., et al., *Hantavirus structure - Molecular interactions behind the scene*. 2012, Microbiology Society. p. 1631-1644.
13. Vaheri, A., et al., *Uncovering the mysteries of hantavirus infections*. 2013, Nature Publishing Group. p. 539-550.
14. Duehr, J., et al., *Neutralizing monoclonal antibodies against the Gn and the Gc of the andes virus glycoprotein spike complex protect from virus challenge in a preclinical hamster model*. 2020, American Society for Microbiology.
15. Acuña, R., et al., *Acidification triggers Andes hantavirus membrane fusion and rearrangement of Gc into a stable post-fusion homotrimer*. 2015, Microbiology Society. p. 3192-3197.
16. Brown, K.S., et al., *Vesicular Stomatitis Virus-Based Vaccine Protects Hamsters against Lethal Challenge with Andes Virus*. 2011, American Society for Microbiology. p. 12781-12791.
17. Prescott, J., et al., *Long-Term Single-Dose Efficacy of a Vesicular Stomatitis Virus-Based Andes Virus Vaccine in Syrian Hamsters*. 2014, Multidisciplinary Digital Publishing Institute. p. 516-523.
18. Safronetz, D., et al., *Adenovirus Vectors Expressing Hantavirus Proteins Protect Hamsters against Lethal Challenge with Andes Virus*. 2009, American Society for Microbiology. p. 7285-7295.
19. Brocato, R., et al., *DNA Vaccine-Generated Duck Polyclonal Antibodies as a Postexposure Prophylactic to Prevent Hantavirus Pulmonary Syndrome (HPS)*. 2012, Public Library of Science. p. e35996.
20. Custer, D.M., et al., *Active and Passive Vaccination against Hantavirus Pulmonary Syndrome with Andes Virus M Genome Segment-Based DNA Vaccine*. 2003, American Society for Microbiology (ASM). p. 9894.
21. Haese, N., et al., *Antiviral Biologic Produced in DNA Vaccine/Goose Platform Protects Hamsters Against Hantavirus Pulmonary Syndrome When Administered Post-exposure*. 2015, Public Library of Science. p. e0003803.
22. Hooper, J.W., et al., *DNA vaccine-derived human IgG produced in transchromosomal bovines protect in lethal models of hantavirus pulmonary syndrome*. 2014, American Association for the Advancement of Science.
23. Hooper, J.W., et al., *DNA Vaccination with the Hantaan Virus M Gene Protects Hamsters against Three of Four HFRS Hantaviruses and Elicits a High-Titer Neutralizing Antibody Response in Rhesus Monkeys*. 2001, American Society for Microbiology. p. 8469-8477.
24. Brocato, R.L. and J.W. Hooper, *Progress on the prevention and treatment of hantavirus disease*. 2019, MDPI AG.
25. de Carvalho Nicacio, C., et al., *Cross-Protection against Challenge with Puumala Virus after Immunization with Nucleocapsid Proteins from Different Hantaviruses*. 2002, American Society for Microbiology. p. 6669-6677.
26. Martinez, V.P. and P.J. Padula, *Induction of protective immunity in a syrian hamster model against a cytopathogenic strain of andes virus*. 2012, John Wiley & Sons, Ltd. p. 87-95.
27. Yin, J., et al., *Select what you need: A comparative evaluation of the advantages and limitations of frequently used expression systems for foreign genes*. 2007, Elsevier. p. 335-347.
28. Schmidt, F.R., *Recombinant expression systems in the pharmaceutical industry*. 2004, Springer. p. 363-372.
29. Demain, A.L. and P. Vaishnav, *Production of recombinant proteins by microbes and higher organisms*. 2009, Elsevier. p. 297-306.
30. Andersen, D.C. and L. Krummen, *Recombinant protein expression for therapeutic applications*. 2002, Elsevier Current Trends. p. 117-123.
31. Duckert, P., S. Brunak, and N. Blom, *Prediction of proprotein convertase cleavage sites*. 2004, Oxford Academic. p. 107-112.
32. Sonnhammer, E.L.L., G. Von Heijne, and A. Krogh, *A hidden Markov model for predicting transmembrane helices in protein sequences*. 1998.
33. Petersen, T.N., et al., *SignalP 4.0: discriminating signal peptides from transmembrane regions*. 2011, Nature Publishing Group. p. 785-786.
34. Gupta, R. and S. Brunak, *Prediction of glycosylation across the human proteome and the correlation to protein function*. 2002. p. 310-322.
35. *Pichia Protocols*, J.M. Cregg, Editor. 2007, Humana Press.
36. Engvall, E. and P. Perlmann, *Enzyme-linked immunosorbent assay (ELISA) quantitative assay of immunoglobulin G*. 1971, Pergamon. p. 871-874.
37. Livak, K.J. and T.D. Schmittgen, *Analysis of relative gene expression data using real-time quantitative PCR and the 2-ΔΔCT method*. 2001, Academic Press Inc. p. 402-408.
38. Wong, M.L. and J.F. Medrano, *Real-Time PCR for mRNA Quantitation*. 2005, Taylor & Francis. p. 75-85.
39. Beltrán-Ortiz, C.E., et al., *Expression and purification of the surface proteins from Andes virus*. 2017, Academic Press. p. 63-70.
40. Ruusala, A., et al., *Coexpression of the membrane glycoproteins G1 and G2 of Hantaan virus is required for targeting to the Golgi complex*. 1992, Academic Press. p. 53-64.
41. Hepojoki, J., et al., *Interactions and Oligomerization of Hantavirus Glycoproteins*. 2010, American Society for Microbiology. p. 227-242.

42. Deyde, V.M., et al., *Interactions and trafficking of Andes and Sin Nombre Hantavirus glycoproteins G1 and G2*. 2005, Academic Press. p. 307-315.
43. Cifuentes-Muñoz, N., N. Salazar-Quiroz, and N.D. Tischler, *Hantavirus Gn and Gc Envelope Glycoproteins: Key Structural Units for Virus Cell Entry and Virus Assembly*. 2014, Multidisciplinary Digital Publishing Institute. p. 1801-1822.
44. Rissanen, I., et al., *Structural Transitions of the Conserved and Metastable Hantaviral Glycoprotein Envelope*. 2017, American Society for Microbiology.
45. Sperber, H.S., et al., *Self-association and subcellular localization of Puumala hantavirus envelope proteins*. 2019, Nature Publishing Group. p. 1-15.
46. Battisti, A.J., et al., *Structural Studies of Hantaan Virus*. 2011, American Society for Microbiology. p. 835-841.
47. Acuña, R., et al., *Hantavirus Gn and Gc Glycoproteins Self-Assemble into Virus-Like Particles*. 2014, American Society for Microbiology. p. 2344-2348.
48. Levanov, L., et al., *Defining of MAbs-neutralizing sites on the surface glycoproteins Gn and Gc of a hantavirus using vesicular stomatitis virus pseudotypes and site-directed mutagenesis*. 2019, Microbiology Society. p. 145-155.
49. Li, S., et al., *A Molecular-Level Account of the Antigenic Hantaviral Surface*. 2016, Elsevier B.V. p. 959-967.
50. Shi, X. and R.M. Elliott, *Analysis of N-Linked Glycosylation of Hantaan Virus Glycoproteins and the Role of Oligosaccharide Side Chains in Protein Folding and Intracellular Trafficking*. 2004, American Society for Microbiology. p. 5414-5422.
51. Shental-Bechor, D. and Y. Levy, *Effect of glycosylation on protein folding: A close look at thermodynamic stabilization*. 2008, National Academy of Sciences. p. 8256-8261.
52. Shental-Bechor, D. and Y. Levy, *Folding of glycoproteins: toward understanding the biophysics of the glycosylation code*. 2009, Elsevier Current Trends. p. 524-533.
53. Hilleman, M.R., *Yeast recombinant hepatitis B vaccine*. 1987, Springer-Verlag. p. 3-7.
54. Barr, E. and G. Tamms, *Quadrivalent human papillomavirus vaccine*. 2007, Oxford Academic. p. 609-617.
55. Chang, J.C.C., et al., *Adjuvant activity of incomplete Freund's adjuvant*. 1998, Elsevier. p. 173-186.
56. O'Hagan, D.T., et al., *The history of MF59® adjuvant: a phoenix that arose from the ashes*. 2013, Taylor & Francis. p. 13-30.
57. Mbow, M.L., E. De Gregorio, and J.B. Ulmer, *Alum's adjuvant action: grease is the word*. 2011, Nature Publishing Group. p. 415-416.
58. Mbow, M.L., et al., *New adjuvants for human vaccines*. 2010, Elsevier Current Trends. p. 411-416.
59. Siddiqui, M.A.A. and C.M. Perry, *Human papillomavirus quadrivalent (types 6, 11, 16, 18) recombinant vaccine (Gardasil®)*. 2006, Springer. p. 1263-1271.
60. Szarewski, A., *HPV vaccine: Cervarix*. 2010, Taylor & Francis. p. 477-487.
61. Hooper, J.W., et al., *A Lethal Disease Model for Hantavirus Pulmonary Syndrome*. 2001, Academic Press. p. 6-14.
62. Milazzo, M.L., et al., *Maporal Viral Infection in the Syrian Golden Hamster: A Model of Hantavirus Pulmonary Syndrome*. 2002, Oxford Academic. p. 1390-1395.
63. Miao, J., et al., *Syrian Hamster as an Animal Model for the Study on Infectious Diseases*. 2019, Frontiers Media S.A. p. 457882.
64. Dienz, O. and M. Rincon, *The effects of IL-6 on CD4 T cell responses*. 2009, Academic Press. p. 27-33.
65. O'Garra, A., *Cytokines induce the development of functionally heterogeneous T helper cell subsets*. 1998, Cell Press. p. 275-283.
66. O'Garra, A. and N. Arai, *The molecular basis of T helper 1 and T helper 2 cell differentiation*. 2000, Elsevier. p. 542-550.
67. Sieling, P.A., et al., *IL-12 regulates T helper type 1 cytokine responses in human infectious disease.* 1994, American Association of Immunologists. p. 3639-3647.
68. Zivcec, M., et al., *Validation of assays to monitor immune responses in the Syrian golden hamster (Mesocricetus auratus)*. 2011, Elsevier. p. 24-35.
69. Kim, S.H. and Y.S. Jang, *The development of mucosal vaccines for both mucosal and systemic immune induction and the roles played by adjuvants*. 2017, The Korean Vaccine Society. p. 15-21.
70. McElrath, M.J., *Adjuvants: Tailoring humoral immune responses*. 2017, Lippincott Williams and Wilkins. p. 278-284.
71. Zhang, L., W. Wang, and S. Wang, *Effect of vaccine administration modality on immunogenicity and efficacy*. 2015, Informa Healthcare. p. 1509-1523.